Supporting Information

Kounitsky et al. 10.1073/pnas.1422843112

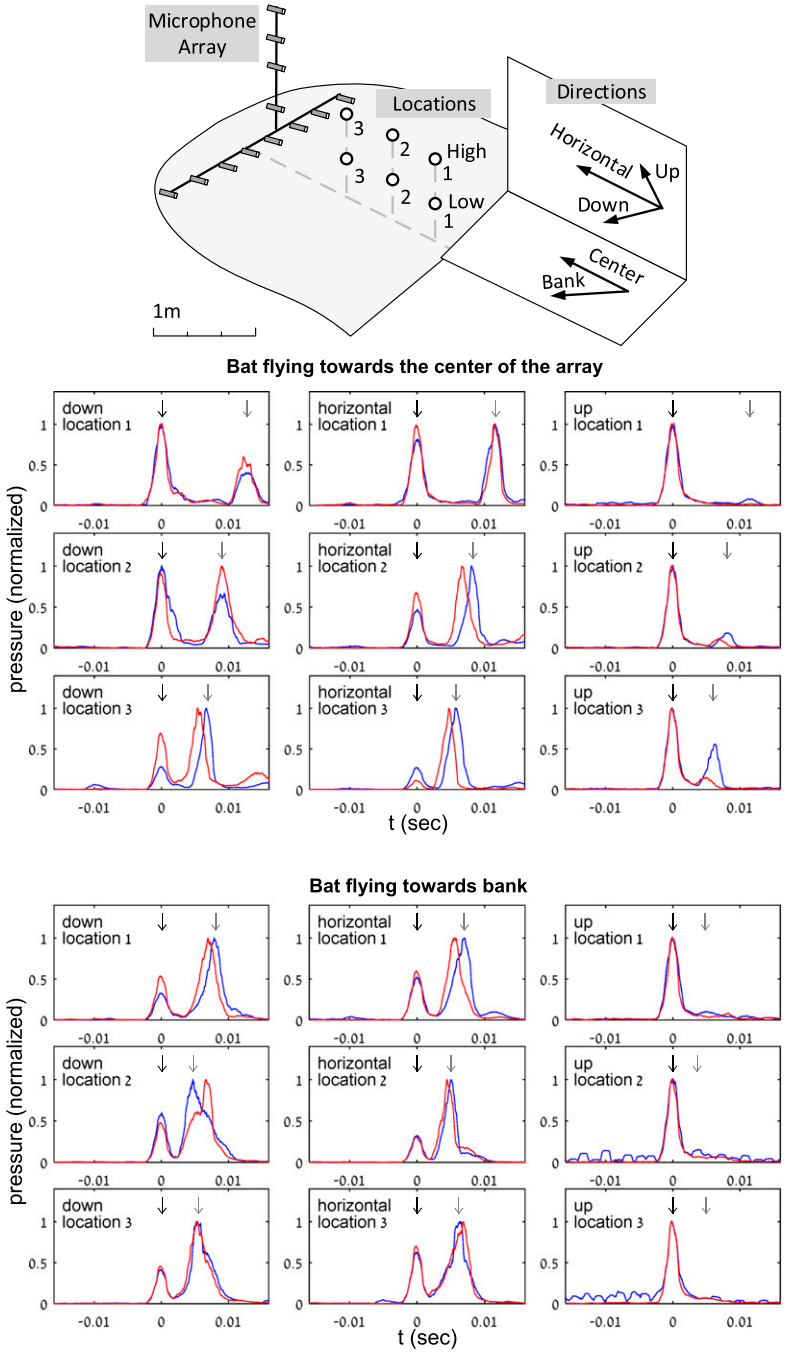

Fig. S1. Assessing environmental clutter (ensonifications). (*Top*) Schematic of the setup showing the positions of the speaker (six positions in two heights) simulating a bat flying toward the array at one of two heights. Direction arrows show the elevations in which the speaker was pointed (up, down, and horizontal representing an ascending, descending, or horizontally flying bat). Lower arrows (bank vs. center) show the azimuth of the simulated bat. We simulated two azimuths: toward the center of the array (center) and toward the left bank (bank). These azimuths were the two directions in which bats mostly flew. (*Middle*) Nine panels show the recordings for a bat flying with a center azimuth. The peak at time 0 is the emitted signal, and the second peak is the echo (both are depicted by arrows). Red and blue show two recordings for two different heights (lower and higher, respectively). The envelope of the time signal is presented. Each time signal was normalized to a maximum of one. Each row shows a different location along the simulated trajectory, and each column shows one elevation. Results clearly show that, when the bat was pointing downward or horizontally, it received a strong echo, whereas when it pointed upward, the echo was minimal. This difference is independent of the location or the azimuth, which can be learned from *Bottom*, which shows the same results for the bank azimuth.

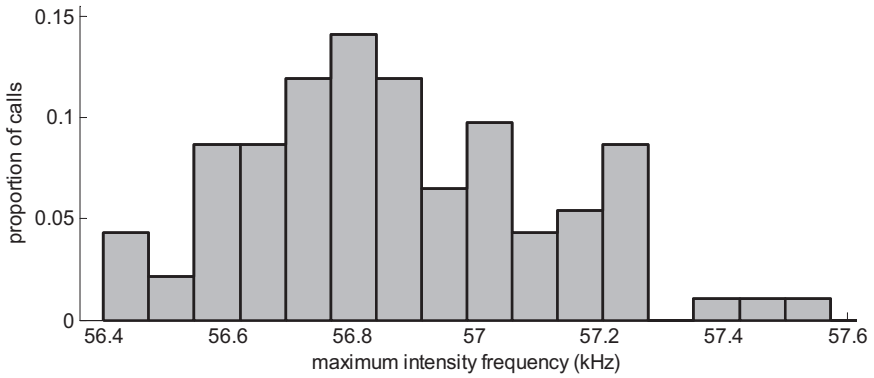

Fig. S2. Pulse frequency histogram (n = 101 pulses; mean = 56.9 kHz; SD = 0.24 kHz). Pulse frequency was calculated using instantaneous frequency analysis (1). The frequency with most intensity is presented.

1. Gardner TJ, Magnasco MO (2006) Sparse time-frequency representations. *Proc Natl Acad Sci USA* 103(16):6094–6099.

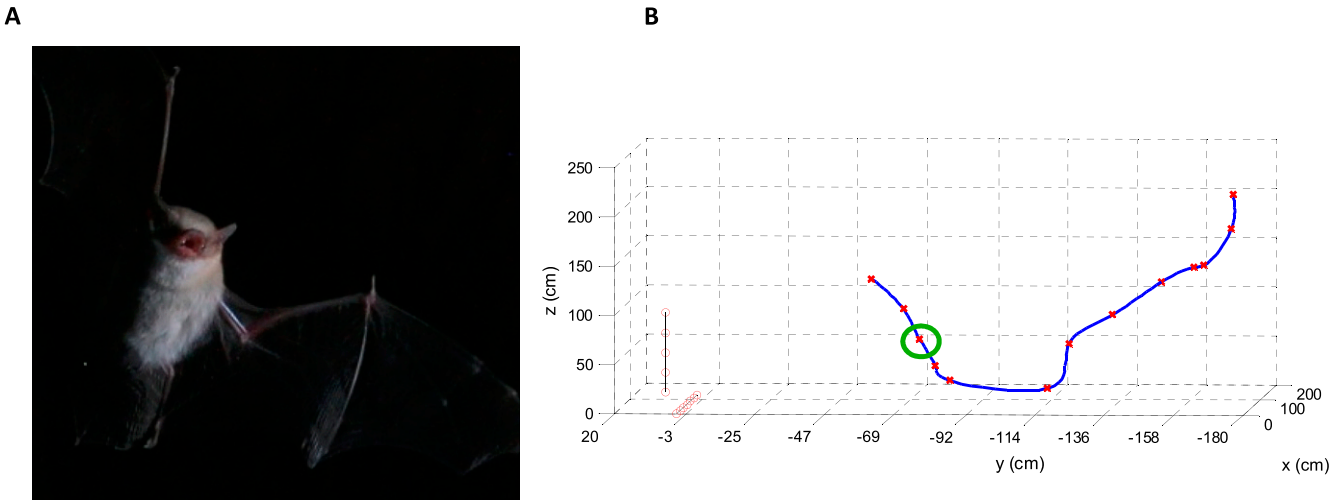

Fig. S3. All analyzed beams were centered within the borders of the array. (*A*) During most ascents, the bats' heads were pointing below the direction of their bodies (and the direction of flight). For example, in this image, the bat is ascending almost parallel to the camera, whereas its mouth is almost perpendicular to the camera. This behavior allowed us to analyze data even in very high-ascending angles. (*B*) The same trial shown in Fig. 1*D* from a different angle, proving that the bat was lower than the top-most microphone, even when emitting the last analyzed call (green circle). As explained in *A*, the bat's gaze in this case was much lower than the direction of its flight.

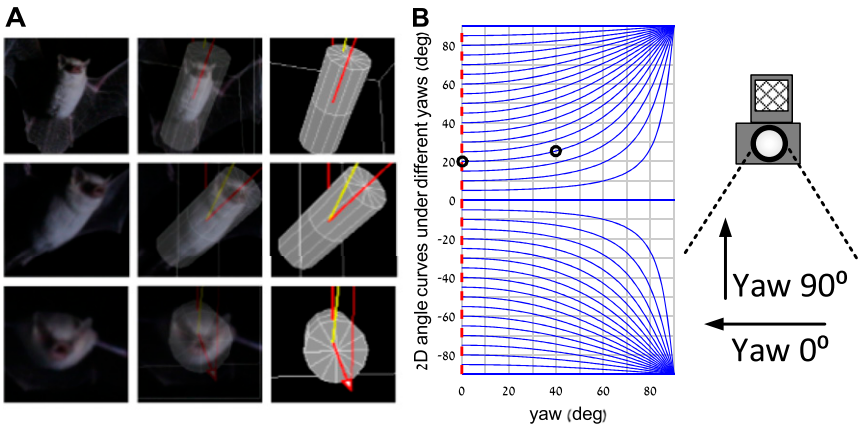

Fig. S4. Correcting for yaw when estimating flight angle. (*A*) The bat's yaw was estimated. This procedure is shown for three different yaw angles: (*Top*) 72°, (*Middle*) 31°, and (*Bottom*) 86°. (*B*) The 3D–2D correcting function was calculated by simulating different 3D flight angles (from −90° to 90°) and changing the yaw toward the camera (from 0° to 90°; camera diagram in *Right*). Each curve represents a particular 3D angle that would be measured in 2D under different yaws. The red line shows yaw 0° (when the bat body is seen to its full length and the measured angle equals to the real angle). Black points describe an example where measured a flight angle of 25° and yaw of 40° is mapped to 20°.